The Plant Cell, Vol. 20: 1330–1345, May 2008, www.plantcell.org

An Exocyst Complex Functions in Plant Cell Growth in *Arabidopsis* and Tobacco [W]

Michal Hála,[a,1] Rex Cole,[b,1] Lukáš Synek,[a] Edita Drdová,[a] Tamara Pečenková,[a,c] Alfred Nordheim,[d] Tobias Lamkemeyer,[d] Johannes Madlung,[d] Frank Hochholdinger,[e] John E. Fowler,[f] and Viktor Žárský[a,c,2]

[a] Institute of Experimental Botany, Academy of Sciences of the Czech Republic, 165 02 Prague 6, Czech Republic
[b] Molecular and Cellular Biology Program, Oregon State University, Corvallis, Oregon 97331
[c] Department of Plant Physiology, Faculty of Science, Charles University, 128 44 Prague 2, Czech Republic
[d] Proteom Centrum Tübingen, Interfaculty Institute for Cell Biology, University of Tübingen, 72076 Tübingen, Germany
[e] Center for Plant Molecular Biology, Department of General Genetics, University of Tübingen, 72076 Tübingen, Germany
[f] Department of Botany and Plant Pathology, Center for Genome Research and Biocomputing, Oregon State University, Corvallis, Oregon 97331

The exocyst, an octameric tethering complex and effector of Rho and Rab GTPases, facilitates polarized secretion in yeast and animals. Recent evidence implicates three plant homologs of exocyst subunits (SEC3, SEC8, and EXO70A1) in plant cell morphogenesis. Here, we provide genetic, cell biological, and biochemical evidence that these and other predicted subunits function together in vivo in *Arabidopsis thaliana*. Double mutants in exocyst subunits (*sec5 exo70A1* and *sec8 exo70A1*) show a synergistic defect in etiolated hypocotyl elongation. Mutants in exocyst subunits SEC5, SEC6, SEC8, and SEC15a show defective pollen germination and pollen tube growth phenotypes. Using antibodies directed against SEC6, SEC8, and EXO70A1, we demonstrate colocalization of these proteins at the apex of growing tobacco pollen tubes. The SEC3, SEC5, SEC6, SEC8, SEC10, SEC15a, and EXO70 subunits copurify in a high molecular mass fraction of 900 kD after chromatographic fractionation of an *Arabidopsis* cell suspension extract. Blue native electrophoresis confirmed the presence of SEC3, SEC6, SEC8, and EXO70 in high molecular mass complexes. Finally, use of the yeast two-hybrid system revealed interaction of *Arabidopsis* SEC3a with EXO70A1, SEC10 with SEC15b, and SEC6 with SEC8. We conclude that the exocyst functions as a complex in plant cells, where it plays important roles in morphogenesis.

INTRODUCTION

Vesicle traffic both through the eukaryotic endomembrane system and to the plasma membrane is facilitated by tethering factors (reviewed in Sztul and Lupashin, 2006; Cai et al., 2007). They act as molecular bridges that provide an initial interaction between the vesicle and its target membrane. This tethering occurs prior to the pairing of SNAREs (soluble N-ethylmaleimide–sensitive attachment protein receptors) and the final fusion of the vesicle with the membrane. In addition to assisting the positioning of the vesicle at the membrane, tethering factors, in combination with Rab GTPases (small GTPases of the Ras superfamily), help to determine the specificity of vesicle targeting. Two general types of tethering factors are recognized: long putative coiled-coil proteins generally occurring as dimers (e.g., Uso1p and p115) and large multisubunit protein complexes (e.g., the exocyst, COG, GARP, HOPS, TRAPPI, and TRAPPII complexes). Of these, the targeting and tethering of Golgi-derived secretory vesicles to the plasma membrane is associated specifically with the exocyst, an eight-protein complex also known as the Sec6/8 complex.

The cellular role of the exocyst has been extensively studied in yeast and animals (reviewed in Hsu et al., 2004). In these eukaryotes, the exocyst is required when physiological or developmental circumstances demand extensive exocytosis to support rapid polarized growth, such as budding in *Saccharomyces cerevisiae* (TerBush and Novick, 1995), hyphal tip growth in *Candida albicans* (Li et al., 2007), the outgrowth of cultured neurites (Hazuka et al., 1999; Pommereit and Wouters, 2007), and membrane trafficking to the leading edge of migrating mammalian epithelial cells (Rosse et al., 2006; Zuo et al., 2006).

The complex of proteins that make up the exocyst was originally described in yeast (TerBush et al., 1996), and, based on sequence homology, the mammalian exocyst was subsequently characterized (Hsu et al., 1996; Kee et al., 1997). In both yeast and mammals, the exocyst complex consists of eight subunits: Sec3, Sec5, Sec6, Sec8, Sec10, Sec15, Exo70, and Exo84 (Hsu et al., 1996; TerBush et al., 1996; Guo et al., 1999a; Matern et al., 2001). Molecular masses of exocyst subunits range from 70 to 140 kD, forming an 834- and 743-kD complex in yeast and mammals, respectively (Hsu et al., 1996; TerBush et al., 1996).

[1] These authors contributed equally to this work.
[2] Address correspondence to zarsky@ueb.cas.cz.
The authors responsible for distribution of materials integral to the findings presented in this article in accordance with the policy described in the Instructions for Authors (www.plantcell.org) are: John E. Fowler (fowlerj@science.oregonstate.edu) and Viktor Žárský (zarsky@ueb.cas.cz).
[W] Online version contains Web-only data.
www.plantcell.org/cgi/doi/10.1105/tpc.108.059105

Although overall sequence identity among different exocyst subunits is <10%, all subunits are predicted to contain similar helical bundles assembled into long rod-like domains (Whyte and Munro, 2001; Dong et al., 2005; Wu et al., 2005; Hamburger et al., 2006; Sivaram et al., 2006). The predicted rod-like domains have recently been verified by crystallography for four of the subunits (reviewed in Munson and Novick, 2006).

Interactions between subunits of the complex in yeast and mammals have been detected by various methods, including yeast two-hybrid assays, coimmunoprecipitation, and pull-down assays (Roth et al., 1998; Guo et al., 1999a, 1999b; Matern et al., 2001; Vega and Hsu, 2001; Moskalenko et al., 2003; Dong et al., 2005; Sivaram et al., 2005). Nevertheless, the exocyst structure and precise mechanism of in vivo exocyst assembly remain unknown. Since the original discovery that the exocyst is an effector of the Rab GTPase Sec4p in yeast (Guo et al., 1999b), several exocyst subunits have been shown to interact with small GTPases of the Rab, Rho, Arf, and Ral families, which help regulate exocyst assembly and/or function in yeast and animals (Adamo et al., 1999; Guo et al., 1999a, 2001; Robinson et al., 1999; Brymora et al., 2001; Zhang et al., 2001, 2004; Moskalenko et al., 2002, 2003; Prigent et al., 2003). Thus, the exocyst appears to play a central role in the mechanism by which small GTPases regulate vesicle trafficking.

Research investigating the exocyst in plants has only recently been reported. Systematic surveys of published plant genomes have identified in silico homologs to all eight exocyst subunits (Cvrckova et al., 2001; Jurgens and Geldner, 2002; Elias et al., 2003). Most of the putative plant exocyst genes exist as multiple copies, compared with the single copies that predominate in other eukaryotes (Elias et al., 2003; Synek et al., 2006). An important role of the exocyst in plant morphogenesis is beginning to emerge from research characterizing mutations of individual plant exocyst components. In maize (*Zea mays*), a transposon insertion into a *SEC3* homolog results in the *roothairless1* mutation, which causes the failure of root hairs to elongate properly (Wen and Schnable, 1994; Wen et al., 2005). *Arabidopsis exo70A1* mutants exhibit a root hair phenotype that is remarkably similar to that of the maize *roothairless1* mutant. They also display other defects in cell growth (e.g., hypocotyl elongation) and reduced cell number (Synek et al., 2006). *Arabidopsis thaliana sec8* mutants demonstrate a defect in the germination and tip growth of pollen tubes (Cole et al., 2005). Intriguingly, electron tomographic analysis of cell plate formation during cytokinesis in *Arabidopsis* uncovered the existence of 24-nm-long structures that tether membrane vesicles (Otegui and Staehelin, 2004; Segui-Simarro et al., 2004). These structures resemble the mammalian exocyst as observed with the electron microscope (Hsu et al., 1998). Recently, interaction of a putative plant exocyst subunit with a small GTPase was demonstrated: *Arabidopsis* SEC3 interacts with plant-specific Rho GTPases (ROPs) via binding to the adaptor protein ICR1 in vivo (Lavy et al., 2007). These studies implicate plant exocyst components in polarized growth, a role that mirrors the one demonstrated in other eukaryotes, but do not demonstrate the existence of the exocyst as a complex in plants.

Here, we combine data from genetic, cell biological, and biochemical analyses to provide evidence that the plant exocyst subunits work in concert to form a functional complex, essential in both the sporophyte and the male gametophyte for plant cell growth. In the pollen tube, our data suggest that the complex is crucial for maintaining the efficient and tightly focused functioning of the growth machinery (termed the localization enhancing network, self-sustaining [LENS] in Cole and Fowler, 2006) at the tube tip.

RESULTS

Weak Mutations in Two Exocyst Components Enhance the exo70A1 Hypocotyl Elongation Defect in Etiolated Seedlings

Although strong mutant alleles of the two exocyst subunit genes tested to date cause severe sporophytic (*EXO70A1*; Synek et al., 2006) or gametophytic (*SEC8*; Cole et al., 2005) defects in *Arabidopsis*, exocyst subunit mutations without phenotypic effects have also been isolated. We hypothesized that if a plant exocyst complex exists in vivo, then combining weak alleles could produce a phenotype that is more severe than that observed for each of the individual mutant alleles alone (i.e., a synergistic effect due to functional interaction). To test this prediction, we evaluated hypocotyl elongation in etiolated *Arabidopsis* seedlings harboring mutations both in *EXO70A1* and in a second exocyst gene. The *exo70A1-1* and *-2* mutations are null alleles that significantly reduce the number and length of hypocotyl cells in etiolated seedlings, resulting in a shortened hypocotyl (Synek et al., 2006) (Figure 1A; $P < 0.001$). An *exo70A1* mutation was combined with either the partially functional *sec8-4* allele (Cole et al., 2005; Table 1) or the *sec5a-1* allele (likely to be a null allele for one of the two genes encoding the SEC5 subunit; see below). In contrast with *exo70A1*, single mutant homozygotes for either *sec8-4* or *sec5a-1* do not display an aberrant phenotype during vegetative development. However, the combination of either of these mutations with a mutation of *exo70A1* resulted in a more severe reduction of hypocotyl elongation in etiolated seedlings than the *exo70A1* mutation alone (Figure 1; $P < 0.001$ for both combinations). A similar result was obtained when the second partially functional *SEC8* allele (*sec8-6*) was combined with *exo70A1-2* (see Supplemental Figure 1 online), arguing that this phenotypic enhancement is due to properties of the gene products and not of particular alleles. Such synergism indicates a functional relationship between these putative exocyst complex components.

Exocyst Subunit Mutations Are Transmitted at a Reduced Rate through the Pollen

Mutants in *Arabidopsis SEC8* locus have a gametophytically expressed pollen defect, resulting in reduced transmission of the mutant alleles through the male (Cole et al., 2005). We hypothesized that if an exocyst complex functions in the male gametophyte, then mutations in other components of the complex should also have a male-specific transmission defect. To test this prediction, we focused our genetic studies on those exocyst genes that appear in the *Arabidopsis* genome as single copies (*SEC6* and *SEC8*) or as two-copy genes that are not tandemly

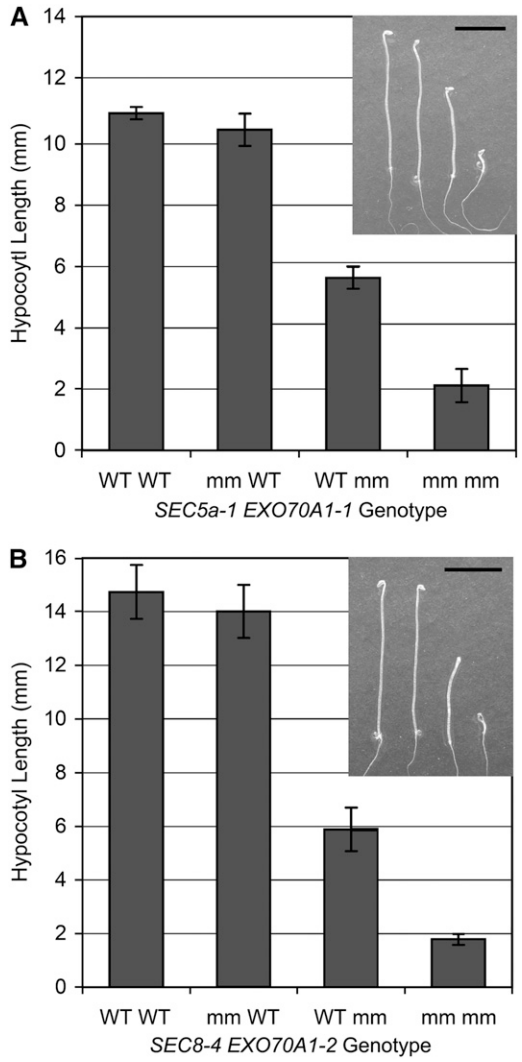

Figure 1. Mutations in Two Different Exocyst Components Show a Synergistic Effect on Hypocotyl Elongation in 5-d-Old Etiolated Seedlings.

(A) Comparison of hypocotyl lengths of siblings that differ with respect to *SEC5a* and *EXO70A1* genotypes. WT denotes plants that are homozygous wild-type or heterozygous for the gene of interest; mm denotes plants that are homozygous mutants. Shown are data for wild-type plants (WT WT, $n = 76$), plants homozygous for the *sec5a-1* mutation alone (mm WT, $n = 25$), plants homozygous for the *exo70A1-1* mutation alone (WT mm, $n = 53$), and plants homozygous for both the *sec5a-1* and *exo70A1-1* mutations (mm mm, $n = 8$).

(B) Analogous results for *sec8-4* and *exo70A1-2* mutations (WT WT, $n = 22$; mm WT, $n = 16$; WT mm, $n = 33$; mm mm, $n = 10$). Error bars indicate SE. Inset are photos of representative dark-grown hypocotyls arranged in the same order of genotypes as in the graphs. Bar = 5 mm.

arranged (*SEC5a/b* and *SEC15a/b*). Initially, *SEC10* was included in this list, but bioinformatic analysis along with analyses of several insertion alleles showed that this locus consists of two tandemly repeated genes (M. Elias, personal communication). Transmission frequencies were determined for T-DNA insertion mutants of exocyst genes *SEC6*, *SEC15a*, *SEC5a*, and *SEC5b* as well as for the *sec5a-1 sec5b-1* double mutant. Each mutant allele was reciprocally outcrossed to wild-type plants for at least three generations (Table 1). In each instance, the mutant allele was transmitted through the female gametophyte at the expected frequency. However, in outcrosses, neither of the two independent mutant alleles (for *SEC6* and *SEC15a*) was transmitted through the pollen. Similarly, the *sec5a-1* and *sec5b-1* alleles were never transmitted through the pollen together, although neither single mutation demonstrated a transmission defect (Table 1), likely reflecting a redundant function for these genes in pollen.

The transmission defect of the *sec6-1* and *sec6-2* mutants was complemented by expression of the wild-type *SEC6* coding sequence driven by the pollen-specific *LAT52* promoter (see Supplemental Figure 2 and Supplemental Table 1 online), as had been previously demonstrated for *sec8-1* and *sec8-3* using *LAT52:SEC8* (Cole et al., 2005). RT-PCR assessment of RNA extracted from plants homozygous for the *SEC5a*, *SEC5b*, or *SEC15a* mutant alleles indicates that these do not produce full-length transcripts (see Supplemental Figure 3 online). (The *SEC15a* homozygous mutants arose at low frequencies from unassisted self-crosses of heterozygotes, likely due to decreased pollen competition in such crosses [Cole et al., 2005].) The altered *SEC5a*, *SEC5b*, and *SEC15a* transcripts are predicted to encode truncated proteins that appear likely to be functionally impaired. Overall, the genetic evidence demonstrates that strong mutations in any of four putative complex components, SEC5, SEC6, SEC8, or SEC15a, result in a similar severe pollen-specific transmission defect. Furthermore, the molecular evidence suggests that this phenotype is associated with null, or near-null, alleles.

Mutations in SEC6, SEC8, SEC15a, and SEC5 Dramatically Affect Both Pollen Germination and Pollen Tube Growth

We were interested to know if the transmission defect observed for components of the putative exocyst complex was associated with similar pollen developmental phenotypes. The male-specific transmission defect in *SEC8* mutants is associated with defects in pollen germination and pollen tube growth (Cole et al., 2005). However, limitations in the earlier studies (e.g., no homozygous plants were available for the most severe *SEC8* alleles) prevented determination of the null phenotype in the pollen tube. To overcome these limitations, representative alleles for each of the four exocyst components with transmission defects were crossed into the *quartet1* (*qrt1*) background. In the *qrt1* background, all four products of a meiosis remain attached to each other (e.g., exactly two wild-type and two mutant pollen grains from a heterozygous plant), allowing direct observation of phenotypes in severe gametophytic mutants (Preuss et al., 1994; Johnson-Brousseau and McCormick, 2004).

Staining of mature pollen from plants homozygous for the *qrt1* mutation and heterozygous for mutations in *SEC6*, *SEC8*, or *SEC15a* with 4′,6-diamidino-2-phenylindole revealed two sperm cell nuclei and a vegetative nucleus in each of the pollen grains in a quartet, and none of the grains showed obvious developmental defects. This indicates that none of these mutations severely affects early pollen grain development, including its mitotic divisions.

Table 1. Outcross Data Indicate That Mutations in Any of the Four Putative Exocyst Genes Evaluated Result in a Pollen-Specific Transmission Defect

	Pollen Donor: +/m					Pollen Donor: +/+				
	Pollen Recipient: +/+					Pollen Recipient: +/m				
Allele	*n*	+/+	+/m	χ^2	P	*n*	+/+	+/m	χ^2	P
(Expected)		50%	50%				50%	50%		
sec5a-1	86	42%	58%	2.28	NS[a]	86	47%	53%	0.214	NS
sec5b-1	117	48%	52%	0.42	NS	117	45%	55%	1.034	NS
sec6-1	79	100%	0%	79	<0.0001	82	50%	50%	0.000	NS
sec6-2	88	100%	0%	88	<0.0001	80	48%	53%	0.200	NS
sec8-1[b]	150	100%	0%	150	<0.0001	157	47%	53%	0.516	NS
sec8-3[b]	105	100%	0%	105	<0.0001	101	50%	50%	0.010	NS
sec8-4[b]	577	82%	18%	235.9	<0.0001	157	51%	49%	0.057	NS
sec8-6[b]	157	69%	31%	22.1	<0.0001	159	52%	48%	0.308	NS
sec15a-1	99	100%	0%	99	<0.0001	100	56%	44%	1.440	NS
sec15a-2	62	100%	0%	62	<0.0001	62	44%	56%	1.032	NS
	Pollen Donor: +/m;+/m					Pollen Donor: +/+; +/+				
	Pollen Recipient: +/+; +/+					Pollen Recipient: +/m;+/m				
Allele	*n*	(+/+;+/m), (+/m;+/+), or (+/+;+/+)	+/m;+/m	χ^2	P	*n*	(+/+;+/m), (+/m;+/+), or (+/+;+/+)	+/m;+/m	χ^2	P
(Expected)		75%	25%				75%	25%		
sec5a-1 *sec5b-1*	185	99.5%	0.5%	58.6	<0.0001	190	72.6%	27.4%	0.568	NS

[a] NS, not significantly different from expected.
[b] Previously published data for *sec8* mutant alleles (Cole et al., 2005) are included for comparison.

To assess for a germination defect, pollen from *qrt1* plants that were heterozygous for a mutation in *SEC6*, *SEC8*, or *SEC15a* was germinated in vitro and compared with the pollen of a *qrt1* sibling lacking the exocyst mutation. Due to the 2:2 distribution of the wild type versus mutant, germination of three or four pollen grains in a quartet from a heterozygote requires the germination of one or both mutant pollen grains. Thus, a pollen germination defect would reduce the relative frequency of quartets with three or four grains germinated. Indeed, we found that the *sec6-1*, *sec6-2*, *sec8-1*, *sec8-3*, *sec15a-1*, and *sec15a-2* mutant alleles were associated with a significant reduction ($P < 0.001$) in the percentage of germinating quartets with three or four grains germinated, compared with their wild-type siblings (mutant frequencies, 1 to 7%; wild-type frequencies, 10 to 30%; Table 2). Only quartets from heterozygotes harboring the weak *sec8-4* allele were not significantly different from the wild type.

Pollen containing mutations of both *SEC5* genes was studied by generating plants that were homozygous for *sec5a-1* and heterozygous for *sec5b-1* in the *qrt1* background. These were compared with pollen from *qrt1* siblings that had a mutation either in only one of the *SEC5* genes or in neither. The frequency of quartets having three and four pollen grains germinating was not significantly affected by either single mutant (*sec5a-1*: 18%, $n = 367$; *sec5b-1*: 22%, $n = 223$; wild type: 23%, $n = 635$). By contrast, pollen from plants homozygous for *sec5a-1* and heterozygous for *sec5b-1* demonstrated a severe germination defect, with only 1.8% of quartets having three or four grains germinated (Table 2).

These analyses revealed that, although mutation of any of the four exocyst components dramatically reduced germination, mutant grains can occasionally produce a pollen tube. Despite the rarity of such events, the arrangement of pollen into quartets allowed us to identify a defective phenotype associated with the mutant pollen tubes by assessing pollen tube length and width in quartets with at least three germinated grains. In all such cases, one or (rarely) two aberrant pollen tubes were observed (Figures 2B to 2E). The length and width of the shortest tube in quartets with three or four germinated grains from mutant heterozygotes (or *sec5a-1* homozygous; *sec5b-1* heterozygous plants) and their corresponding wild-type siblings were determined. For all four exocyst components, the mutants were associated with significantly shorter and thicker pollen tubes than the shortest pollen tubes produced by the wild type ($P < 0.001$, $n = 22$ to 44 for each genotype) (Figures 2G and 2H). In addition, mutant pollen tubes were only 15 to 25% as long as the average wild-type pollen tube, whereas the length of the longer tubes in these same quartets closely resemble the wild type (Figure 2I). The aberrant pollen tubes were occasionally irregularly shaped (e.g., Figure 2E), with the observed range of shapes similar for all mutations evaluated. Again, only in *sec8-4* quartets were the pollen tubes morphologically indistinguishable from the wild type (Figures 2F to 2H). Taken together, these data show that mutation of each of

Table 2. Percentage of Germinating Quartets with Three or Four Grains Germinated

	Genotype of Pollen Source					
	Wild Type		Heterozygous			
Allele	n[a]	% 3 or 4	n[a]	% 3 or 4	χ^2	P
sec5a sec5b[b]	635	23.1	227	1.8	54.51	<0.001
sec6-1	809	12.0	607	4.0	28.66	<0.001
sec6-2	944	20.3	1086	7.4	70.35	<0.001
sec8-1	518	29.7	652	3.1	162.09	<0.001
sec8-3	760	21.7	655	1.2	137.63	<0.001
sec15a-1	606	12.4	972	3.7	42.93	<0.001
sec15a-2	301	10.3	175	1.7	11.72	<0.001
sec8-4	576	13.4	741	11.2	1.43	NS[c]

[a] Number of germinating quartets evaluated.
[b] The pollen source for *sec5a sec5b* was heterozygous for *sec5b* and homozygous for *sec5a*.
[c] NS, not significantly different from expected ($P < 0.05$).

four putative exocyst components, SEC6, SEC8, SEC15a, or SEC5, results in similar developmental defects in both pollen germination and polarized pollen tube growth.

Colocalization of Exocyst Subunits at the Tip of Growing Pollen Tubes

Defects in pollen germination and pollen tube growth observed in *Arabidopsis* exocyst subunit mutants imply a common function for these proteins in pollen tube germination and tip growth. If acting as a complex, all exocyst subunits should show some overlapping localization in vivo. Subunit localization was investigated using indirect immunofluorescence in tobacco (*Nicotiana tabacum*) pollen tubes, taking advantage of their larger size and more robust in vitro germination. Mouse polyclonal antibodies raised against recombinant *Arabidopsis* proteins SEC6 and EXO70A1 and a rabbit polyclonal antibody raised against an *Arabidopsis* SEC8 peptide all recognized homologs of these subunits in tobacco (see Supplemental Figure 5B online). Preimmune sera for these antibodies showed a very weak homogenous background signal lacking any specific pattern (see Supplemental Figure 4 online).

As predicted, based on a function in pollen tube tip growth, all three antibodies revealed predominant tip-focused localization of the exocyst subunits that they recognize (Figure 3). Bright tiny dots forming a granular pattern could be discerned within the apical signal. Behind the intense signal at the tip, the staining is much weaker. However, sparse small spots are also distributed in the cytoplasm and especially along the plasma membrane within the entire tube length.

We took advantage of the distinct sources for anti-SEC8 (rabbit) versus anti-EXO70A1 and anti-SEC6 (mouse) and demonstrated colocalization of SEC8 and EXO70 proteins and SEC8 and SEC6 proteins, respectively, by double labeling (Figures 3G and 3H). We initially observed that only the SEC6 signal was visible in the tip of pollen tubes when labeled by both anti-SEC6 and anti-SEC8 simultaneously, even though either antibody stained the tip when used alone (Figures 3C to 3F). When the procedure was adjusted such that anti-SEC8 was added first, followed by the addition of anti-SEC6 1 h later, both labels were visualized at the pollen tube tip (Figure 3H). One possible explanation for these observations is that the SEC6 antibody spatially blocks the epitope recognized by the SEC8 antibody due to close association of these two components within the exocyst complex.

When we examined subcellular distribution of SEC6 and SEC8 in germinating tobacco pollen, we observed a maximum of the signal in the 100,000*g* pellet fraction (Figure 4) containing all postnuclear membranes. In both cases, only weak signal was observed in the cytosolic fraction. Moreover, the signal increased in both cases during the first 60 min of pollen germination, indicating simultaneous accumulation of exocyst subunits in the membrane fraction and implying de novo synthesis of these subunits.

Overall, we conclude that the exocyst subunits SEC6, SEC8, and EXO70 have an overlapping localization pattern predominantly at the tips of growing pollen tubes. This localization pattern is consistent with a role indicating their close spatial interaction to facilitate the intensive exocytosis at that site.

Chromatographic Fractionation Reveals That the Plant Exocyst Complex Exists as a Biochemical Entity

Shared pollen phenotypes, colocalization at the growing pollen tube tip, and the synergism of mutations in the reduction of hypocotyl elongation provide strong, but indirect, evidence that the exocyst subunits form a functional exocyst complex in plants. We adapted chromatography methods previously used to successfully characterize the exocyst complex in yeast and mammalian cells (Hsu et al., 1996; TerBush et al., 2001) to provide more direct evidence for the existence of the exocyst complex as a biochemical entity in plant cells. Because an *Arabidopsis* suspension culture in its exponential growth phase expresses exocyst subunit genes at high mRNA levels (see Supplemental Figure 8 online), this cell type was chosen as a source for exocyst complex purification. Also, preliminary experiments showed cosedimentation of the putative complex with the microsomal fraction after centrifugation at 100,000*g* (Figure 4). Therefore, we used a crude total cell lysate depleted of heavy membranes but containing microsomes for our chromatographic analyses.

To detect the complex subunits, we used the three antibodies already described above (anti-EXO70A1, anti-SEC6, and anti-SEC8) as well as anti-SEC3, anti-SEC5, and anti-SEC15a (see Supplemental Figure 5A online). Duplication of genes encoding several of the exocyst subunits in the *Arabidopsis* genome raises a question about antibody specificity. Based on high sequence similarity, we expect that polyclonal antibodies against SEC3 and SEC5 recognize both isoforms of respective subunits. Because the polyclonal anti-SEC15a was prepared against a peptide specific for SEC15a, we do not expect cross-reactivity with SEC15b. Conversely, we have confirmed using an *exo70A1* mutant that the EXO70A1 antibody is specific to EXO70A1 (at least in the sporophyte), as it does not recognize any other proteins on protein gel blots (see Supplemental Figure 5C online).

We initially performed size exclusion gel chromatography (SEGC) on a HiLoad SUPERDEX 200 column. When the resultant

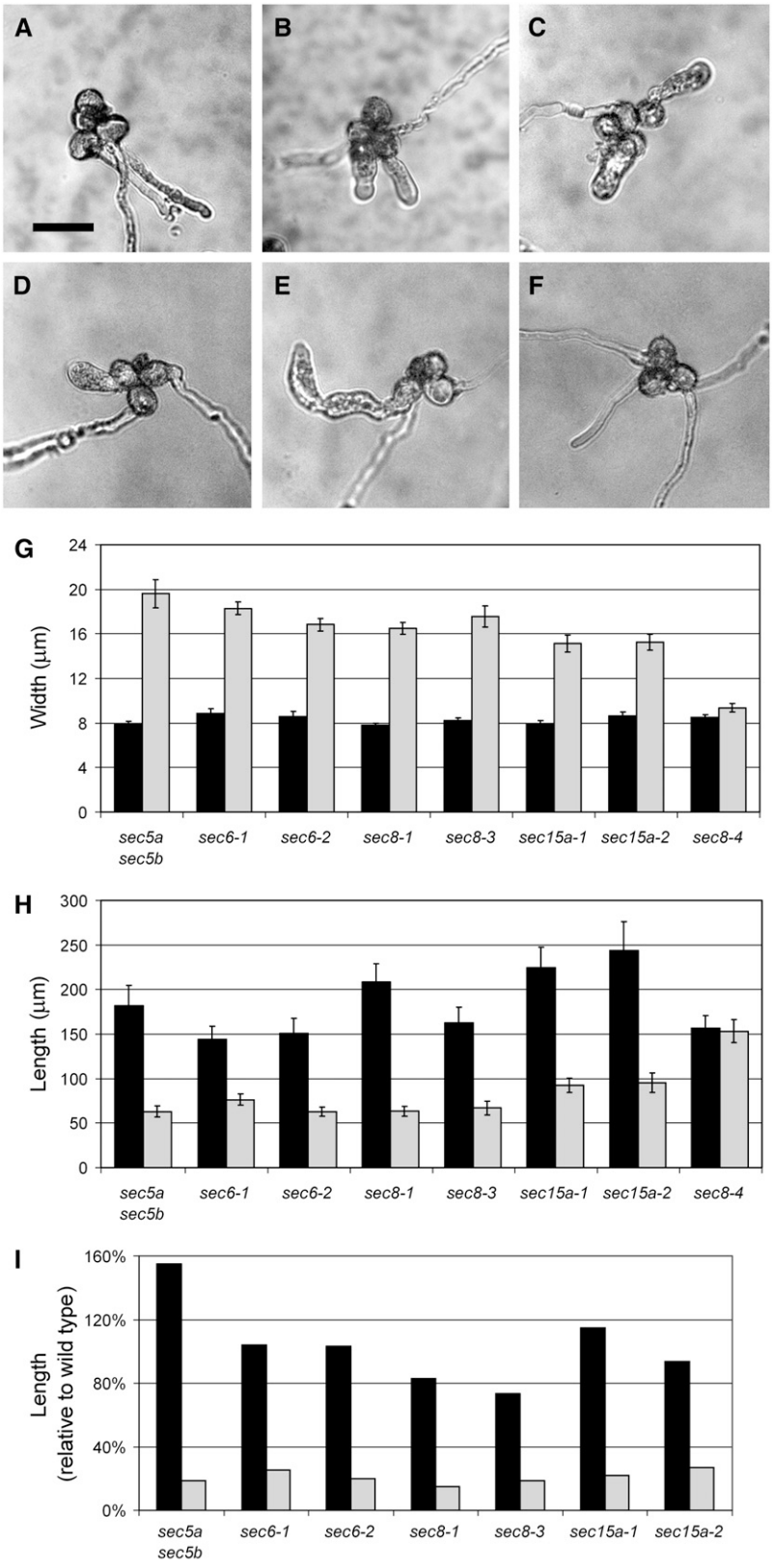

Figure 2. Exocyst Mutants Share a Similar Aberrant Pollen Tube Phenotype.

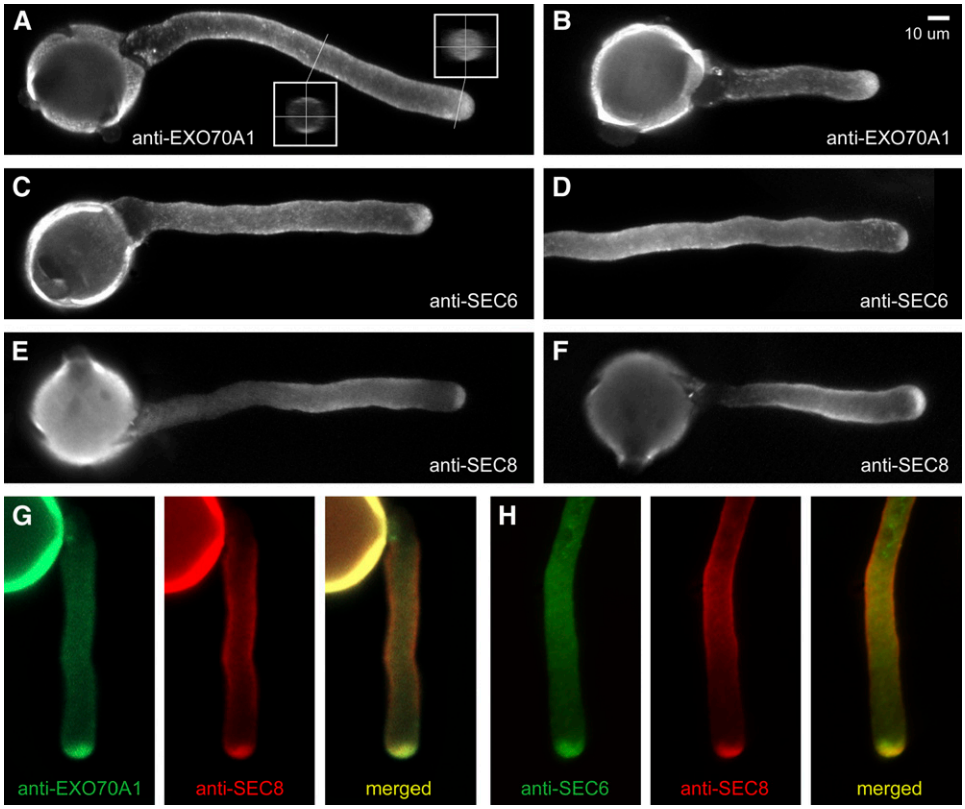

Figure 3. Localization of EXO70, SEC6, and SEC8 to the Tip in Tobacco Pollen Tubes by Indirect Immunofluorescence.

(A) and **(B)** Projections of confocal sections labeled by the EXO70A1 antibody. Transverse sections through the pollen tube made by three-dimensional reconstruction are displayed.
(C) and **(D)** Projections of confocal sections labeled by the SEC6 antibody.
(E) and **(F)** Projections of confocal sections labeled by the SEC8 antibody.
(G) Double labeling by mouse EXO70A1 antibody and rabbit SEC8 antibody shows colocalization of these subunits at the tip of pollen tubes.
(H) Double labeling by mouse SEC6 antibody and rabbit SEC8 shows colocalization of these subunits at the tip of pollen tubes.

protein fractions were subjected to SDS-PAGE and protein gel blotting, most of the exocyst subunits were detected in high molecular mass fractions. Figure 5A shows that signals of all polyclonal antibodies form peaks with a maximum in the same fractions, suggesting a complex size of ~900 kD. These peaks are well behind the total protein maximum (Figure 5A), suggesting specific enrichment of all putative exocyst subunits detected in these fractions. Incubation of the total lysate with 0.5 M phosphate in the lysis buffer led to similar results after SEGC, SDS-PAGE, and protein gel blots, suggesting that the presence of phosphate does not affect complex stability (data not shown).

Figure 2. (continued).

(A) to **(F)** Germinated *qrt1* pollen from wild-type plants compared with the *qrt1* pollen from sibling plants mutated in putative exocyst component genes. Each panel is identified by the genotype of the parent. Bar = 50 μm.
(A) Homozygous wild type with respect to exocyst genes.
(B) Homozygous for *sec5a-1* and heterozygous *sec5b-1.*
(C) Heterozygous for *sec6-1.*
(D) Heterozygous for *sec8-3*.
(E) Heterozygous for *sec15a-1*.
(F) Heterozygous for *sec8-4*.
(G) to **(I)** Dimensions of aberrant pollen tubes in *qrt1* pollen from plants heterozygous for an exocyst mutation compared with pollen tubes in the *qrt1* pollen from wild-type siblings. Error bars indicate SE.
(G) Widths of aberrant pollen tubes from exocyst mutants (gray) compared with widths of shortest tubes in quartets of wild-type siblings (black).
(H) Lengths of aberrant pollen tubes from exocyst mutants (gray) compared with the lengths of the shortest tubes in quartets of wild-type siblings (black).
(I) Length of aberrant pollen tubes (gray) and nonaberrant pollen tubes (black) in quartet pollen from plants heterozygous for an exocyst mutation, relative to the length of all pollen tubes measured in wild-type siblings (n = 76 to199).

We next employed three-step purification based on the method described by Hsu et al. (1996) to purify the mammalian exocyst. We started with high-capacity affinity chromatography on polyphosphate hydroxyapatite matrix (hydroxyapatite Bio-Gel) with discontinuous phosphate elution. All fractions were subjected to SDS-PAGE, protein gel blotting, and analyzed by anti-SEC6 and anti-SEC8 antibodies. Corresponding fractions containing both SEC6 and SEC8 were collected and prepared for the second purification step by dialysis. In the second purification step, the dialyzed fractions from the affinity chromatography were loaded onto an ion exchange chromatography column (Fractogel EMD-TMAE). All expected subunits of *Arabidopsis* exocyst have a calculated pI under 7, with values ranging mostly between 5.2 and 5.8. Anex resin was then used to isolate the exocyst complex in the buffer with almost neutral pH. Fractions containing exocyst antibody signals were eluted with the salt concentration between 0.35 and 0.42 M. Protein gel blot analysis of these fractions demonstrated a weakened signal for the SEC5 and especially SEC15a proteins, possibly due to a partial loss of these subunits during this purification step.

The fractions obtained from ion exchange chromatography were then subjected to SEGC and protein gel blot analysis to complete the third step of the purification. Figure 5B shows that the distribution of the antibody signals demonstrates again cofractionation of exocyst subunits. All signals had only one maximum, and this occurred in fractions corresponding to a molecular mass of 750 kD. Consistent with a smaller mass for the three-step purified complex, SEC15a could not be detected, and the SEC5 signal was very weak, requiring substantially longer exposure time. This observation suggests that some subunits may form a stable core of the complex, whereas other subunits (e.g., SEC15a and SEC5) are more loosely associated, at least under these experimental conditions. Importantly, cofractionation of five exocyst subunits (SEC3, SEC5, SEC6, SEC8, and EXO70A1) was maintained through all three steps of purification.

To complement identification of exocyst subunits by protein gel blot analysis following partial purification, we used liquid

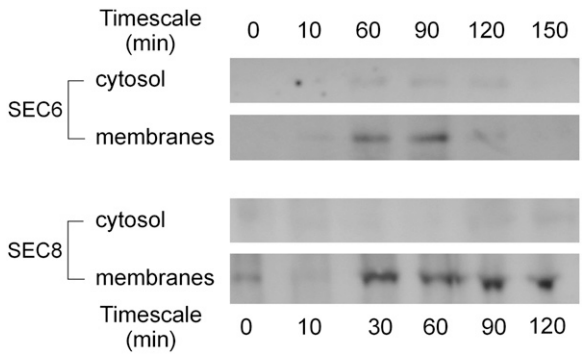

Figure 4. Accumulation of SEC6 and SEC8 in Germinating Tobacco Pollen.

N. tabacum (cv Samsun) pollen was incubated in 10% sucrose and 0.01% boric acid for the time periods described. Cytosolic and membrane fractions (100,000*g* pellet) were loaded on 10% SDS-PAGE, 50 μg of total protein per lane, and assayed by protein gel blot analysis using anti-SEC6 and anti-SEC8 antibodies.

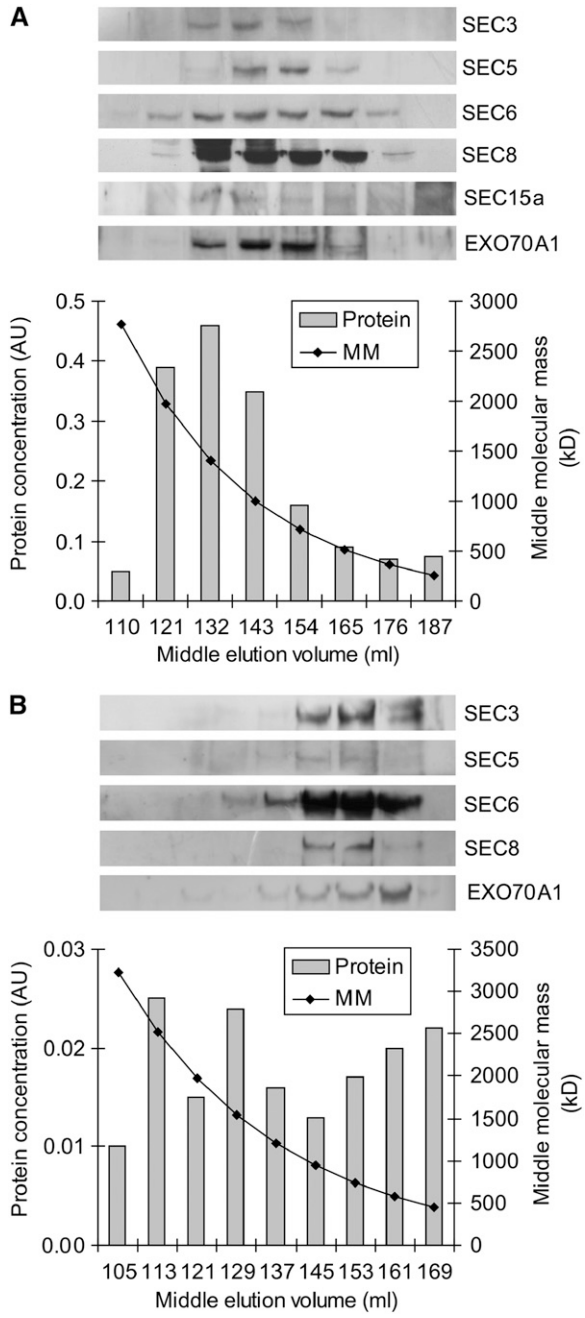

Figure 5. Cofractionation of Exocyst Subunits in Column Chromatography.

(A) SEGC of total protein extract from *Arabidopsis* suspension culture. Shown is the cofractionation of exocyst subunits in SEGC fractions as detected with exocyst-specific antibodies.

(B) SEGC as the third purification step of the same extract, following hydroxyapatite affinity chromatography and ion exchange chromatography. Shown is the cofractionation of exocyst subunits in high molecular fractions of SEGC as detected with exocyst-specific antibodies.

Top panels in **(A)** and **(B)** show protein gel blot analyses. Columns in bottom panels of **(A)** and **(B)** show relative total protein concentration measured with a UV detector at 254 nm. MM indicates approximate middle molecular mass calculated for each 5-mL fraction.

chromatography electrospray ionization tandem mass spectrometry (LC-ESI-MS/MS) to analyze protein bands of expected molecular masses following the three-step purification (see Supplemental Figure 6 online). This approach confirmed that the exocyst-positive fractions (by protein gel blot) contain the SEC3a, SEC6, and SEC8 subunits. In addition, SEC10 (for which we had no antibody) was also identified in these fractions (see Supplemental Table 2 online). Taken together, using a combination of analytic methods we demonstrated that SEC3, SEC5, SEC6, SEC8, SEC10, SEC15, and EXO70A1 were components of the same protein complex (for EXO84, see Discussion).

Blue Native Electrophoresis and the Yeast Two-Hybrid Assay Provide Independent Support for the *Arabidopsis* Exocyst

To confirm data obtained from the chromatographic approach, we employed two additional methods. First, we used a blue native PAGE (BN-PAGE) technique that is based on a mild solubilization in detergent and treatment with the dye Coomassie Brilliant Blue G 250 (Schägger and von Jagow, 1991; Berghöfer and Klösgen, 1999; Werhahn and Braun, 2002). After the solubilization with the mild detergent dodecyl-β-D-maltoside (DDM) in concentrations of total protein to DDM ratio of 1.33 and low NaCl concentrations (10 and 30 mM), a range of high molecular mass complexes was detected for four of the five exocyst complex components tested: SEC3, SEC6, SEC8, and EXO70A1 (see Supplemental Figure 7A online). Under the conditions of higher detergent concentrations (total protein:DDM ratio of 0.67) and no additional salt, SEC6 and EXO70A1 were predominantly present in small, rather than in high, molecular complexes (see Supplemental Figure 7B online). Notably, we observed a well-defined complex detected only by anti-SEC6 that could represent SEC6 dimers. By contrast, the SEC3 subunit was still found in larger complexes under these conditions, although running at a lower mass than at lower detergent concentrations. Again, this is consistent with loss of some subunits (e.g., SEC6 and EXO70) from the complex under certain conditions (see Discussion).

To further support complex formation, the interaction abilities of one of each type of the expected exocyst subunits were tested using the yeast two-hybrid assay. We used the GAL4 system, based on the split GAL4 transcription factor controlling expression of reporter genes (Figure 6). We found that SEC3a, SEC10, and EXO84b showed high activation capacity when fused with the DNA binding domain alone and thus were unsuitable as bait proteins in this assay; EXO84b also showed promiscuous interactions when fused with the activation domain. However, we observed three pairs of strongly interacting subunits: EXO70A1/SEC3a, SEC15b/SEC10, and SEC6/SEC8 (Figure 6). All three pairs were confirmed by β-galactosidase assay and by the double auxotrophic marker.

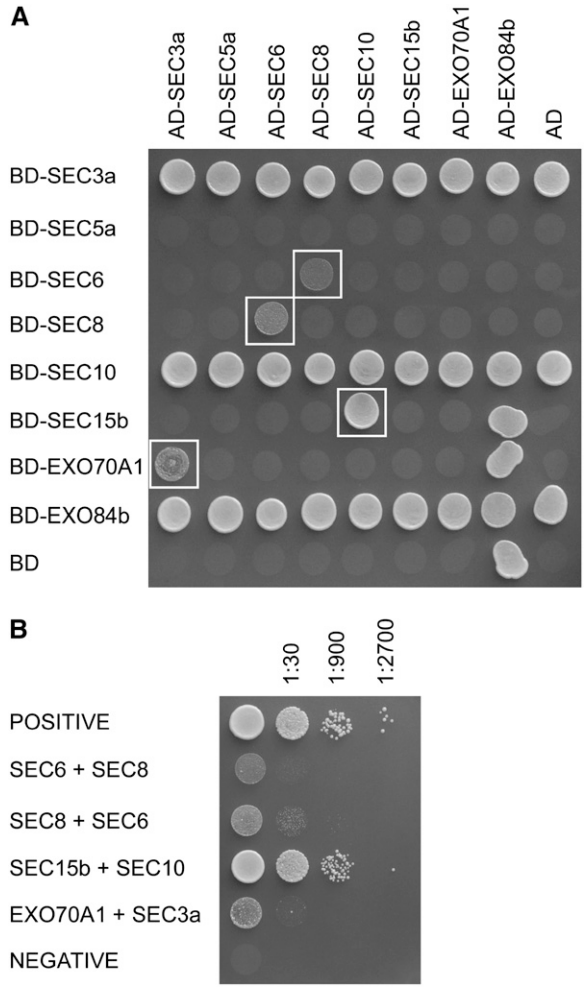

Figure 6. Yeast Two-Hybrid Analysis of Pairwise Interactions of Exocyst Subunits.

(A) Pairwise interaction of all exocyst subunits. Lines and columns describe fusion forms of exocyst subunits used for transformation. Single colonies were resuspended in 150 μL of sterile water and dropped on selective plates, and each drop was 10 μL. Yeast strain AH109 was grown on -ADE-HIS-LEU-TRP plates at 28°C. Combinations boxed by white squares also showed positive β-galactosidase activity. BD, the DNA binding domain; AD, the activation domain.

(B) Strength of interaction compared with a positive control (see Methods). Single colonies were resuspended in 150 μL of sterile water. Serial dilutions 1:30, 1:900, and 1:2700 in sterile water were prepared and dropped on -ADE-HIS-LEU-TRP plates at 28°C, and each drop was 10 μL.

DISCUSSION

In model non-plant eukaryotic cells, such as yeast, *Drosophila melanogaster*, mouse, rat, and human, the octameric exocyst complex facilitates the targeting and tethering of secretory vesicles to the plasma membrane and thereby is integral to a broad range of physiological processes requiring polarized exocytosis. Comparative genomic and phylogenetic analysis across 17 eukaryote genomes suggests that the exocyst, like the other tethering complexes, is ancient, originating very early in eukaryotic evolution (Koumandou et al., 2007). The existence of such a complex in plants has been anticipated by the discovery that genes orthologous to those encoding the eight exocyst components in yeast and mammals are present in several plant genomes and are expressed in *Arabidopsis* and rice (*Oryza*

sativa). Here, we have provided biochemical evidence, supported by genetic analysis, phenotypic observations, and cell biological experiments, to conclude that the exocyst does indeed function as a complex in plants. The results of these various approaches, shown with respect to the putative complex subunits, are summarized in Table 3.

Composition of the Plant Exocyst Complex

Size exclusion gel chromatography revealed copurification in a high molecular mass fraction of all exocyst subunits for which antibodies were available, namely, SEC3, SEC5, SEC6, SEC8, SEC15a, and EXO70A1. Mass spectrometry confirmed the presence of SEC3a, SEC6, and SEC8 in the same high molecular mass fraction and moreover identified SEC10, for which we did not have any antibody.

The maxima of all exocyst subunits signals are localized to the same fraction, corresponding to a molecular mass of ~900 kD. However, the predicted size of the plant exocyst is 760 kD, assuming that it contains one member of each subunit, consistent with the characterized exocyst complexes in yeast and mammals (Hsu et al., 1996; TerBush et al., 1996; Kee et al., 1997). A similar observation was made in yeast where the molecular mass of soluble 19.5S particles, later identified as the exocyst complex, was reported to be between 1000 and 2000 kD, although the calculated molecular mass was only 834 kD (Bowser and Novick, 1991; Bowser et al., 1992).

Also, chromatography results indicated the mammalian exocyst to have a molecular mass of 1000 to 1500 kD, compared with the calculated 743 kD (Yeaman et al., 2004). The difference between observed and calculated molecular mass could be explained by association of additional interacting proteins with the complex. For example, E-cadherin coimmunoprecipitates with the mammalian exocyst (Yeaman et al., 2004). In *Arabidopsis*, the ICR1 adaptor protein was recently identified to interact with SEC3, providing a link to activated ROP (Rho of plants) GTPases (Lavy et al., 2007). Therefore, association of such proteins with the exocyst during purification is possible. Alternatively, because changes in protein shape can influence both sedimenatation rate and apparent molecular mass, the larger size indicated by SEGC may simply be a result of the predicted rod-like structure of the exocyst (Hsu et al., 1998; reviewed in Munson and Novick, 2006) inhibiting its mobility through the pores of the size exclusion matrix. Finally, the plant exocyst could have more than one member of each subunit or additional, plant-specific subunit(s). However, the composition of the exocyst and other quatrefoil tethering complexes seems to be highly conserved in evolution (Whyte and Munro, 2002; Koumandou et al., 2007).

Use of a three-step purification process (Figure 5B) resulted in a shift of the exocyst signal maxima toward a lower molecular mass, indicative of a reduction in the size of the complex. We hypothesize that some subunits may form a stable core of the complex that is maintained through the three-step purification, whereas other subunits are more loosely associated, at least under these conditions. Consistent with this hypothesis, higher-salt (0.35 M NaCl) conditions during ion exchange chromatography induced the loss of SEC5 and SEC15a, while leaving the remaining core complex intact. Similarly, results from blue native electrophoresis demonstrated that increasing detergent concentration also destabilizes the complex (see Supplemental Figure 7B online). The yeast exocyst also shows a molecular mass decrease under high salt conditions (0.5 M NaCl) at pH 8.0 (Bowser and Novick, 1991). However, unlike the yeast exocyst (TerBush et al., 2001), the plant exocyst did not demonstrate complex instability in phosphate buffer or at pH 8.0. A range of high molecular mass complexes (>500 kD) associated with exocyst subunits was detected by BN-PAGE, possibly as a result of both the method used and the dynamics of the exocyst structure in plant cells. Thus, BN-PAGE provides independent verification that subunits of the exocyst do form high molecular mass complexes. Moreover, experiments implied the presence of a SEC6 dimer, which is consistent with previous observations in yeast (Sivaram et al., 2005).

Yeast two-hybrid analysis of plant exocyst components revealed strong interactions between SEC3a and EXO70A1,

Table 3. Summary of Evidence for Inclusion of Various Subunits in a Plant Exocyst Complex

Subunit	Genetic Interaction in Sporophyte	Male-Specific Transmission Defect	Pollen Germination and Tube Growth Defect	Immunolocalization at Pollen Tube Tip	SEGC on Crude Extract	Three-Step Purification; Protein Gel Blot	Three-Step Purification; Protein Sequencing	BN-PAGE	Interaction in Yeast Two-Hybrid System
SEC3					+	+	+[a]	+	+[a]
SEC5a/b	+[b]	+[c]	+[c]		+	+			
SEC6		+	+	+	+	+	+	+	+
SEC8	+	+	+	+	+	+	+	+	+
SEC10							+		+
SEC15a/b		+	+		+[d]				+[e]
EXO70A1	+			+	+	+		+	+

[a] SEC3a was identified/used in this experiment.

[b] Interaction only tested with *sec5a* mutant.

[c] Double mutants (*sec5a sec5b*) produce a phenotype different from the wild type; single mutants in either gene are unaffected.

[d] Polyclonal SEC15a antibody likely recognizes only the SEC15a isoform.

[e] SEC15b was used in the two-hybrid assay.

SEC15b and SEC10, and between SEC6 and SEC8. These pairwise interactions are conserved in both yeast and animals, although in yeast, the Sec3p-Exo70p and Sec6p-Sec8p interactions were identified using immunoprecipitation or pull-down assay rather than the two-hybrid assay (Guo et al., 1999a; Matern et al., 2001; Sivaram et al., 2005). Since SEC3a exocyst subunit was shown to interact with the activated ROP GTPases via ICR1 adaptor protein (Lavy et al., 2007), it would be necessary to check not only how promiscuous or specific the SEC3a interaction is with different EXO70s but also whether ICR1-bound SEC3a is able to bind EXO70. Unfortunately, in the case of EXO84 subunit, it turned out that in our two-hybrid analysis it interacted nonspecifically also in controls. We do not have antibodies against EXO84 subunit yet; however, our preliminary data from the mutant allele transmission analysis (see bellow) point to the possibility of pollen transmission defect. We expect that EXO84 is an exocyst subunit also in plants. The overall number of two-hybrid interactions identified so far among plant exocyst subunits in our experiments is similar to those reported for yeast (Guo et al., 1999a) but lower than those reported for animals (Matern et al., 2001). The notion of direct interaction between SEC6 and SEC8 subunits in vivo is further supported by the finding that the SEC6 antibody blocks the labeling of the pollen tube tip by the SEC8 antibody, unless anti-SEC8 is added before anti-SEC6 (Figure 3). Obstruction of the epitope recognized by anti-SEC8 by SEC6 antibody implies that the two proteins are located in close proximity, perhaps with the SEC8 epitope lying deeper within the exocyst structure.

A prerequisite for the exocyst to function as a complex is the colocalization of its components to regions of the cell where it is active (e.g., sites of intensive secretion). We have demonstrated by indirect immunofluorescence that SEC6, SEC8, and EXO70 all localize to such a site, the tobacco pollen tube tip, a region of vigorous polarized exocytosis. Intriguingly, our time-course evaluation of SEC6 and SEC8 accumulation in tobacco pollen shows an increase in both proteins during the first 60 min after germination (Figure 4). Although we cannot discriminate in this experiment whether the exocyst detected in the pellet fraction is membrane bound (Yeaman, 2003), our data clearly show simultaneous accumulation of SEC6 and SEC8 in germinating tobacco pollen. This implies a functional link between these two subunits in polarization of the vegetative cell during pollen grain germination.

It seems that exocyst subunit interactions and complex architecture differ somewhat between animals and yeast (e.g., Guo et al., 1999a; Matern et al., 2001; Moore et al., 2007). Our data for *Arabidopsis* concerning exocyst size, the more labile association of some subunits, and the lack of two-hybrid interactions reported in yeast and animals support the possibility that the exocyst complex of land plants has yet another distinct architecture, perhaps one that allows functional exploitation of the multiple subunit isoforms (Synek et al., 2006) and adaptor proteins encoded by plant genomes (Lavy et al., 2007).

Genetic Analyses Imply an Important Role for the Plant Exocyst in Cell Growth

Yeast null mutants in exocyst genes are nonviable, whereas temperature-sensitive mutants block exocytosis as manifested by accumulation of secretory vesicles in the cytoplasm (Novick et al., 1980; TerBush et al., 1996; Finger and Novick, 1997; Guo et al., 1999a). The knockout of the Sec5 subunit and depletion of the Sec10 mRNA in *Drosophila* resulted in early postembryonic lethality (Andrews et al., 2002; EauClaire and Guo, 2003; Murthy et al., 2003). Similarly, mice with a mutant allele for the Sec8 subunit died during an early stage of embryogenesis (Friedrich et al., 1997). Mutations in both *Drosophila* and mouse Sec15 led to developmental defects caused by affected membrane recycling (Jafar-Nejad et al., 2005; Lim et al., 2005; Garrick and Garrick, 2007).

In plants, genetic analyses of the function of exocyst subunits SEC3, SEC8, and EXO70A1 were already initiated (Cole et al., 2005; Wen et al., 2005; Synek et al., 2006). In this report, we further extended this effort. SEC5, SEC6, SEC8, and SEC15a subunits were most amenable to genetic analysis not only because they are encoded by one- or two-copy genes that are not tandemly duplicated (as are *SEC3* and *SEC10*) but also because T-DNA insertional lines were available for these loci. Mutations in any of these four exocyst components result in a similar pollen-specific transmission defect. By placing the mutant lines in a *qrt1* background, it was possible to observe that each of these mutations is associated in vitro with reduced pollen germination and defective polarized growth of the pollen tube as exemplified by aberrant short and wide pollen tubes. We previously proposed that the exocyst is one component of a network of signaling pathways (the LENS) that acts to focus exocytosis and growth to the tip of pollen tubes and root hairs (Cole and Fowler, 2006). The defective polarized growth of the pollen tube associated with mutations in these four exocyst components supports such a role for the complex, assuming that when any of its subunits is disrupted, the entire complex becomes nonfunctional. However, it should be noted that the aberrant pollen tubes for each of the four mutated subunits retain some polarity. Among known pollen mutants, the exocyst-loss phenotype is perhaps most reminiscent of pollen tubes overexpressing a dominant-negative mutant ROP GTPase (reviewed in Yang, 2002). Although a functional connection between ROP and the exocyst has not

Table 4. List of *Arabidopsis* Mutants Used in This Work

Mutant	AGI Code[a]	Line	Published in
exo70A1-1	At5g03540	SALK_014826	Synek et al. (2006)
exo70A1-2	At5g03540	SALK_135462	Synek et al. (2006)
sec5a-1	At1g76850	SALK_010127	This work
sec5b-1	At1g21170	SALK_001525	This work
sec6-1	At1g71820	SALK_078235	This work
sec6-2	At1g71820	SALK_072337	This work
sec8-1	At3g10380	SALK_057409	Cole et al. (2005)
sec8-3	At3g10380	SALK_026204	Cole et al. (2005)
sec8-4	At3g10380	SALK_118129	Cole et al. (2005)
sec8-6	At3g10380	SALK_091118	Cole et al. (2005)
sec15a-1	At3g56640	SALK_006302	This work
sec15a-2	At3g56640	SALK_067498	This work
exo84b	At5g49830	GABI_459C01	This work
qrt1	At5g55590	CS8050	Preuss et al. (1994)

[a] AGI, Arabidopsis Genome Initiative.

been shown in pollen, the linkage between them in vegetative cell polarized growth (activated ROP interacts with SEC3 via ICR1; Lavy et al., 2007) makes this an attractive hypothesis.

The existence of a full octameric exocyst complex functioning in plant pollen predicts that mutations or silencing of other exocyst components will demonstrate similar defects. Indeed, our preliminary analyses have revealed equal distribution of heterozygous and wild-type plants in the progeny of self-pollinated *EXO84/exo84b* heterozygotes (wild type, 48%; heterozygous, 52%; homozygous 0%; $n = 120$). Although detailed analysis of these mutants is in progress, this phenotype seems very likely to result from a pollen-transmission defect.

The role of the exocyst in plants is not limited to pollen, as polarly growing root hairs are short in the *rth1* mutant, a maize *SEC3* homolog, and in *Arabidopsis exo70A1* mutants (Wen and Schnable, 1994; Wen et al., 2005; Synek et al., 2006). Mutations in *EXO70A1* also display other defects in cell growth (e.g., etiolated hypocotyl elongation, stigmatic papillae elongation, and reduced cell number) (Synek et al., 2006). We used the *exo70A1*-related defect in hypocotyl elongation to demonstrate that mutations in two exocyst components have a synergistic effect, as would be predicted if the two components are functioning members of the same complex. The observed synergism of the partially functional alleles, *sec8-4*, *sec8-6*, or *sec5a-1*, with an *exo70A1* mutant supports a role for the exocyst complex in sporophytic cell growth.

We also find it noteworthy that the exocyst mutants do not show two other phenotypes that might have been predicted based on earlier evidence. Although there is evidence of exocyst-like structures at the somatic and postmeiotic cell plates in *Arabidopsis* (Otegui and Staehelin, 2004; Segui-Simarro et al., 2004), none of the four strong gametophytic mutants listed in the above paragraph shows evidence of cytokinetic defects during pollen development. In addition, none of these mutants is associated with transmission defects through the female gametophyte, suggesting that the exocyst does not play an essential role in its growth or development.

Finally, despite the fact that EXO70A1 appears to be the predominant EXO70 isoform in *Arabidopsis*, *EXO70A1* is poorly expressed in pollen and mutations in the gene do not cause a transmission defect (see Supplemental Figure 8 online; Synek et al., 2006). *EXO70* proliferated into 23 paralogous genes in *Arabidopsis* (Elias et al., 2003), so it is highly probable that other EXO70 isoforms function as genuine components of the exocyst complex in pollen. Based on analysis of expression data, at least six EXO70 paralogs are transcriptionally active in pollen (Synek et al., 2006). While single-copy plant exocyst genes are expressed in both sporophyte and gametophyte, the multiplied genes typically are expressed at different levels in different tissues, with some overlap in expression of paralogs, particularly of those for *EXO70* (Cole et al., 2005; Synek et al., 2006). This raises the possibility that different plant cells and tissues might be endowed with different versions of the exocyst, each performing specific functions. Consequently, the plant exocyst may have evolved distinctive structures and functions compared with the single complex of fungi and mammals.

Overall, we have demonstrated that an exocyst complex functions in plants, opening the door to investigation of a host of related questions. Data available so far hint that we might expect the involvement of exocyst complex not only in cell growth but also in cell wall formation, meristem regulation, polar auxin transport, and general cell defense against pathogen attack.

METHODS

Plant Material and Growth Conditions

Lines of Columbia-0 ecotype of *Arabidopsis thaliana* with T-DNA insertions and the *qrt1* mutant were obtained from the SALK Institute (Alonso et al., 2003) and GABI-Kat (Rosso et al., 2003). See Table 4 for gene and line codes. The location of each T-DNA insertion within a gene of interest was verified by sequencing from each end of the insert. The *Arabidopsis* suspension culture was derived from vegetative tissue of the Columbia-0 ecotype. For indirect immunofluorescence experiments on pollen, we exploited mature pollen of *Nicotiana tabacum* cv Samsun.

Arabidopsis seeds were surface sterilized, stratified at 4°C for 3 to 5 d, and planted on growth media (1× Murashige and Skoog, 2% [w/v] sucrose, and vitamins) or soil as previously described (Cole et al., 2005). Plants were grown in a climate chamber at 22°C under long-day conditions (16 h of light per day; 7500 lx), with the exception of dark-grown seedlings used in hypocotyl elongation experiments. In the hypocotyl elongation experiments, surface-sterilized, stratified, and plated seeds were placed in a lighted incubator at 22°C for 2 to 4 h to stimulate germination and then wrapped in foil, oriented vertically, and placed in a dark box in the incubator. After 5 d, images of the hypocotyls were captured with a Moticam 1000 camera attached to a Zeiss Stemi SV 11 dissecting microscope. Measurement of hypocotyl lengths was performed from the digital photographs using ImagePro software (MediaCybernetics).

Pollen Germination Experiments

Flowers shedding pollen from *Arabidopsis* plants of the desired genotypes were placed in each well of a 96-well plate (one flower per well) containing 50 μL liquid *Arabidopsis* pollen germination medium [18% sucrose, 0.01% boric acid, 2 mM $CaCl_2$, 1 mM $Ca(NO_3)_2$, and 1 mM $MgSO_4$, with pH adjusted to 6.5 with KOH]. Each plate was incubated at 22°C overnight. A researcher blind to the genotypic source of the flowers microscopically screened the plate for wells with >50% of the quartets showing germinated pollen grains. For these wells, the number of quartets showing one, two, three, or four pollen grains germinated were counted, and images of quartets with three or four grains germinated were captured with a SPOT camera (Diagnostic Instruments) for subsequent measurement of pollen tube widths and lengths with ImagePro software. Staining of ungerminated quartet pollen with 4′,6-diamidino-2-phenylindole was performed as previously described (Cole et al., 2005).

Antibody Preparation

Polyclonal mouse anti-At SEC3a, anti-At SEC5a, and anti-At EXO70A1 were raised against full-length proteins expressed in *Escherichia coli*. The anti-At SEC3a antibody was affinity purified on Ni-NTA agarose according to the manufacturer's protocol (Qiagen). Polyclonal mouse anti-At SEC6 antibody was prepared against truncated At SEC6Δ protein (At SEC6 cDNA cleaved by *Bam*HI and religated).

Polyclonal anti-At SEC8 was raised by synthesis of a peptide (C-LREELARIDESWAAA) corresponding to amino acids 16 to 30 of the predicted *Arabidopsis* protein, conjugation of the peptide to KLH via the N-terminal Cys (C), immunization of rabbits using a standard protocol, and affinity purification of the antibody against the peptide on a column (Genemed Synthesis). Polyclonal anti-At SEC15a was raised against a peptide (CZ-TAKKKSMDMLKKRLKEFN) corresponding to amino acids

772 to 789 (the C terminus) of the predicted *Arabidopsis* protein, which was conjugated to KLH via the N-terminal Cys (C), with the aminocaproic acid (Z) serving as a spacer between the Cys/KLH and SEC15a sequence. Chickens were immunized using a standard protocol, and the antibody was affinity purified against the peptide on a column (Aves Labs).

Indirect Immunofluorescence of Pollen Tubes

Tobacco pollen was cultivated in tobacco pollen germination medium II (10% sucrose and 0.01% H_3BO_3) for 1 h and then fixed with 3.7% formaldehyde in PEM (50 mM PIPES, 5 mM EGTA, and 5 mM $MgSO_4$, pH 6.9) containing 10% sucrose for 1 h (equal volumes of double-concentrated fixation solution and pollen suspension were mixed together). All steps were performed at room temperature unless otherwise specified. After two rinses with PEM and one rinse with PEM/PBS (1:1), pollen was treated with a cell wall–degrading enzyme mix (0.3% cellulase, 0.3% pectinase, and 0.05% pectolyase in PBS) for 20 min. After Tween 20 was added to a final concentration of 0.05%, this preparation was incubated for 10 min. After incubation in 1% BSA in PBS for 30 min, specimens were processed as follows: (1) overnight incubation with primary antibody (mouse anti-SEC6, anti-EXO70A1, and anti-tubulin DM1 [Sigma-Aldrich], or rabbit anti-SEC8, respectively) in PBS containing 1% BSA at 4°C; (2) three rinses in PBS for 10 min; (3) 1-h incubation with FITC-conjugated sheep anti-mouse antibody (Sigma-Aldrich) or TexasRed-conjugated donkey anti-rabbit antibody (Santa Cruz Biotechnology), both diluted 1:150; (4) three rinses in PBS for 10 min. Finally, pollen was mounted into antifade mounting medium (50% glycerol with 0.1% *p*-phenylenediamine in PBS) and observed using an Olympus BX51 fluorescence microscope and a Zeiss LSM 5 Duo confocal laser scanning microscope. The anti-tubulin antibody served as a positive control for the labeling procedure, revealing a pattern of tubulin cytoskeleton typical for tobacco pollen tubes (see Supplemental Figure 3 online).

Chromatographic Purification

Hydroxyapatite Chromatography

Seven-day-old *Arabidopsis* suspension culture cells (90 g) were ground in liquid nitrogen with a mortar and pestle. Then, 1 mL of Sec6/8 buffer (20 mM HEPES, pH 6.8, 150 mM NaCl, 1 mM EDTA, 1 mM DTT, and 0.5% Tween 20) supplemented with 1× protease inhibitor cocktail (Sigma-Aldrich) per 1 g of the fresh weight was added and grinded again. The total lysate was sequentially centrifuged at 5000*g*, 10 min, and 30,000*g*, 30 min at 4°C. Supernatant was then supplemented with 110 mM sodium phosphate (final concentration) and applied to 25 mL hydroxyapatite column (Bio-Rad), which was equilibrated with Sec6/8 buffer supplemented with 110 mM sodium phosphate at room temperature (flow rate 24 mL/h). The column was washed with 70 mL of wash buffer (0.15 M sodium phosphate, pH 7.4, 0.15 M NaCl, and 1 mM DTT), and elution was done in 10 5-mL steps using wash buffer with a sodium phosphate concentration varying between 0.2 and 0.65 M, pH 7.4. Fractions containing exocyst subunits (protein gel blot analysis) were pooled and dialyzed twice against 1 liter of 20 mM Tris, pH 6.8, 100 mM NaCl, 0.2 mM EDTA, and 0.5 mM DTT.

Ion Exchange Chromatography

Dialyzed hydroxyapatite fractions were diluted with the equal volume of 20 mM Tris, pH 6.8, and loaded on the 3-mL Fractogel EMD TMAE (S) column (Merck) equilibrated with 10 mL of 20 mM Tris, pH 6.8, 50 mM NaCl, and 1 mM DTT. The column was then washed with 20 mL of equilibration buffer and eluted with 3 mL fractions containing 150 to 450 mM NaCl (50 mM increment) in equilibration buffer. All was done at 4°C using flow rate of 24 mL/min.

SEGC

Pooled ion exchange chromatography fractions containing exocyst subunits or 80 mg of total protein (in one-step analysis) were applied on an equilibrated (Sec6/8 buffer) Superdex300 HiLoad 26/60 column (Pharmacia) at 4°C with a flow rate 60 mL/min. Protein concentration in eluate was measured with a UV detector (254 nm). Five-milliliter fractions were taken and assayed by protein gel blot analysis.

Protein Gel Blot Analysis

A volume of the sample containing ~30 μg of total protein was acetone precipitated and loaded on 10% SDS-PAGE. Proteins were transferred to a nitrocellulose membrane and blocked overnight with 5% nonfat dry milk in TBS (50 mM Tris-Cl, pH 7.4, and 150 mM NaCl). Primary antibody dilutions in TBS supplemented with 0.5% Tween 20 were as follows: polyclonal mouse anti-At SEC3a, 1:500; polyclonal mouse anti-At SEC5a, 1:1500; polyclonal mouse anti-At SEC6, 1:1000; polyclonal rabbit anti-At SEC8, 1:500; polyclonal chicken anti-At SEC15a, 1:500. Appropriate secondary horseradish peroxidase–conjugated antibodies were applied followed by chemiluminescent ECL detection (SuperSignal; Amersham).

Nano-LC-ESI-MS/MS Mass Spectrometry Analysis

Protein bands were excised from the SDS-PAGE gel in the expected area visible after Coomassie Brilliant Blue staining after the last step (i.e., SEGC fractionation) of the three-step procedure. Excised proteins were digested directly in the gel using trypsin (porcine, sequencing grade, modified; Promega) overnight at 37°C. Reversed-phase nano-LC-MS/MS was performed using an Ultimate nanoflow LC system (Dionex/LC Packings) containing the components Famos (autosampler), Switchos (loading pump and switching valves), and Ultimate (separation pump and UV detector). The LC system was coupled to a QSTAR Pulsar i Hybrid QqTOF mass spectrometer (Applied Biosystems/MDS Sciex) equipped with a nanoelectrospray ion source (Column Adapter [ADPC-PRO] and distal coated SilicaTips [FS360-20-10-D-20]; New Objective).

Briefly, the tryptic peptide mixtures were autosampled at a flow rate of 30 μL/min in 0.1% aqueous trifluoroacetic acid and desalted on a PepMap C18 trapping cartridge (LC Packings). The trapped peptides were eluted and separated on the analytical column (75 μm i.d. × 15 cm; PepMap C18; LC Packings) using a linear gradient of 7 to 50% solvent B (acetonitrile 84% [v/v] in 0.1% [v/v] formic acid) for 27 min at a flow rate of 220 nL/min and ionized by an applied voltage of 2200 kV to the emitter.

The mass spectrometer was operated in data-dependent acquisition mode to automatically switch between MS and MS/MS. Survey MS spectra were acquired for 1.5 s, and the three most intense ions (doubly or triply charged) were isolated and sequentially fragmented for 1.5 s by low-energy collision-induced dissociation. All MS and MS/MS spectra were acquired with the Q2-pulsing function switched on and optimized for enhanced transmission of ions in the MS (m/z 400 to 1000) and MS/MS (m/z 75 to 1300) mass ranges.

Proteins were identified by correlating the ESI-MS/MS spectra with the NCBI.nr-protein sequence database *Viridiplantae* (green plants) as of 07/25/07 using the MOWSE algorithm as implemented in the MS search engine MASCOT (Matrix Science; Perkins et al., 1999). All results from two-dimensional electrophoresis and MS and all search results were stored in a LIMS database (Proteinscape 1.3; Bruker Daltonics).

Blue Native Electrophoresis

Five-day-old *Arabidopsis* cell suspension culture cells (100 mg) were ground in liquid nitrogen to a fine powder, and protein extraction was performed using 100 μL of solubilization buffer (0.5 mM EDTA, 500 mM aminohexanoic acid, 50 mM BisTris, 2 mM PMSF, and protease inhibitor

cocktail [Sigma-Aldrich]) supplied with either 10, 30, or 100 mM NaCl and 0.5 or 1% DDM (Fluka). Additionally, an extraction with no salt added and a ratio of proteins to DDM 0.67 and 1.33 was performed. The protein concentration was determined by the Lowry method (Bio-Rad Dc Protein Assay). Protein samples of ~300 μg were loaded onto 6 to 10% gradient BN-PAGE (6 × 8 cm) gels at 4°C under constant current of 3.5 to 7 mA for 2 to 3 h (Eubel et al., 2005). A mixture of thyroglobulin (670 kD; Sigma-Aldrich) and ferritine (440 kD; Sigma-Aldrich) was used as the marker. Additionally, the plant green tissue extract was used as a marker with distinct chlorophyll binding complexes of ~600 and 150 kD. The individual lanes were cut out, incubated for 30 min with 2% SDS and 2% β-mercaptoethanol, and placed on the top of the 12% SDS-PAGE and assayed by protein gel blot analysis.

Yeast Two-Hybrid System

The yeast two-hybrid screening employed the MATCHMAKER GAL4 Two-Hybrid System 3 (Clontech), and all procedures followed the manufacturer's protocols. The yeast strain AH109 (*MATa*, *trp1-109, leu2-3, 112, ura3-52, his3-200, gal4Δ, gal80Δ*, *LYS2::GAL1*$_{UAS}$*-GAL1*$_{TATA}$*-HIS3, MEL1, GAL2*$_{UAS}$*-GAL2*$_{TATA}$*-ADE2, URA3::MEL1*$_{UAS}$*-MEL1*$_{TATA}$*-lacZ*) was stepwise transformed with all possible combinations of exocyst subunits (*SEC3a*, *SEC5a*, *SEC6*, *SEC8*, *SEC10*, *SEC15b*, *EXO70A1*, and *EXO84b*), fused either with the GAL4 DNA binding domain (pGBKT7vector) or with the GAL4 activation domain (pGADT7 vector). Yeast were grown on -LEU-TRP selective media and then transferred both to -ADE-HIS-LEU-TRP selective media and to filter paper for the β-galactosidase assay. Murine p53 (binding domain) and SV40 large T-antigen (activation domain), provided by the kit manufacturer, were used as a positive control, and a combination of empty pGBKT7 and pGADT7 vectors was used as a negative control. Only combinations positive in β-galactosidase assay and growing on -ADE-HIS-LEU-TRP selective media were accepted as true interactors.

Accession Numbers

Sequence data from this article can be found in the GenBank/EMBL data libraries under following accession numbers. Arabidopsis Genome Initiative codes for *Arabidopsis* loci are also provided in parentheses: At *SEC3a*, NM 103648.2 (At1g47550); At *SEC3b*, NM 103649.2 (At1g47560); At *SEC5a*, AF 479278.1 (At1g76850); At *SEC5b*, NM 101971.2 (At1g21170); At *SEC6*, AF 479279.1 (At1g71820); At *SEC8*, NM 111873.3 (At3g10380); At *SEC10*, AF 479280.1 (At5g12370); At *SEC15a*, NM 115523.1 (At3g56640); At *SEC15b*, NM 116468.3 (At4g02350); At *EXO70A1*, NM 120434.4 (At5g03540); At *EXO84a*, NM 100913.1 (At1g10385); At *EXO84b*, NM124361.4 (At5g49830); At *EXO84c*, NM 100892.2 (At1g10180); At *QRT1*, NM 124941.2 (At5g55590). See also Table 4 for a list of Arabidopsis Genome Initiative locus identifiers, germplasm identification numbers, and references for mutant lines used in this study.

Supplemental Data

The following materials are available in the online version of this article.

Supplemental Figure 1. Comparison of Hypocotyl Lengths of Siblings That Differ with Respect to *SEC8-6* and *EXO70A1-2* Genotypes.

Supplemental Figure 2. Complementation of *sec6* Mutants.

Supplemental Figure 3. Altered Transcripts Predicted to Encode Truncated Proteins in the T-DNA Insertion Mutants in Exocyst Subunits.

Supplemental Figure 4. Negative and Positive Controls Used for Indirect Immunofluorescence on Tobacco Pollen Tubes.

Supplemental Figure 5. Protein Gel Blot Analysis of Exocyst-Specific Antibodies.

Supplemental Figure 6. SDS-PAGE of the SEGC Fraction Containing Partially Purified Exocyst.

Supplemental Figure 7. Blue Native Electrophoresis of the Exocyst Complex from *Arabidopsis* Suspension Culture.

Supplemental Figure 8. Expression Analysis of Exocyst Genes in Different *Arabidopsis* Tissues.

Supplemental Table 1. Genotyping Results for *sec6* Mutant Complementation Experiments.

Supplemental Table 2. ESI-MS Identification of SEC3a, SEC6, SEC8, and SEC10 Exocyst Subunits.

Supplemental Table 3. List of PCR Primers Used in This Work.

ACKNOWLEDGMENTS

We thank Z. Vejlupkova and H. Pham for assistance with *Arabidopsis* growth and genotyping in the lab and the Oregon State University Central Services Lab for sequencing. We also thank F. Cvrckova, M. Elias, M. Fendrych, M. Potocky, and D. Ziak for their practical contributions and comments to the manuscript. Last but not least, we gratefully acknowledge bioinformatic analyses performed by Claudia Fladerer. The work in the lab of V.Z. was supported by the Ministry of Education, Youth, and Sports of the Czech Republic (MSMT Kontakt ME841, MSMT LC06034) and the Grant Agency of the Academy of Sciences of the Czech Republic (IAA6038410). Part of V.Z. income is covered by MSM0021620858. The work in the lab of J.E.F. was supported by the U.S. National Science Foundation (IBN-0420226), which also supported this international collaboration. Work in the lab of F.H. is supported by funds of the Deutsche Forschungsgemeinschaft. The Proteom Centrum Tübingen is supported by the Ministerium für Wissenschaft und Kunst, Landesregierung Baden-Württemberg.

Received February 28, 2008; revised April 16, 2008; accepted May 5, 2008; published May 20, 2008.

REFERENCES

Adamo, J.E., Rossi, G., and Brennwald, P. (1999). The Rho GTPase Rho3 has a direct role in exocytosis that is distinct from its role in actin polarity. Mol. Biol. Cell **10:** 4121–4133.

Alonso, J.M., et al. (2003). Genome-wide insertional mutagenesis of *Arabidopsis thaliana.* Science **301:** 653–657.

Andrews, H.K., Zhang, Y.Q., Trotta, N., and Broadie, K. (2002). Drosophila Sec10 is required for hormone secretion but not general exocytosis or neurotransmission. Traffic **12:** 906–921.

Berghöfer, J., and Klösgen, R.B. (1999). Two distinct translocation intermediates can be distinguished during protein transport by the TAT (Deltaph) pathway across the thylakoid membrane. FEBS Lett. **460:** 328–332.

Bowser, R., Muller, H., Govindan, B., and Novick, P. (1992). Sec8p and Sec15p are components of a plasma membrane-associated 19.5S particle that may function downstream of Sec4p to control exocytosis. J. Cell Biol. **5:** 1041–1056.

Bowser, R., and Novick, P. (1991). Sec15 protein, an essential component of the exocytotic apparatus, is associated with the plasma membrane and with a soluble 19.5S particle. J. Cell Biol. **6:** 1117–1131.

Brymora, A., Valova, V.A., Larsen, M.R., Roufogalis, B.D., and Robinson, P.J. (2001). The brain exocyst complex interacts with RalA in a GFP-dependent manner: Identification of a novel mammalian Sec3 gene and a second Sec15 gene. J. Biol. Chem. **276:** 29792–29797.

Cai, H., Reinisch, K., and Ferro-Novick, S. (2007). Coats, tethers, Rabs, and SNAREs work together to mediate the intracellular destination of a transport vesicle. Dev. Cell **12:** 671–682.

Cole, R.A., and Fowler, J.E. (2006). Polarized growth: Maintaining focus on the tip. Curr. Opin. Plant Biol. **9:** 579–588.

Cole, R.A., Synek, L., Zarsky, V., and Fowler, J.E. (2005). SEC8, a subunit of the putative *Arabidopsis* exocyst complex, facilitates pollen germination and competitive pollen tube growth. Plant Physiol. **138:** 2005–2018.

Cvrckova, F., Elias, M., Hala, M., Obermeyer, G., and Zarsky, V. (2001). Small GTPases and conserved signalling pathways in plant cell morphogenesis: From exocytosis to Exocyst. In Cell Biology of Plant and Fungal Tip Growth, A. Geitmann and M. Cresti, eds (Amsterdam: IOS Press), pp. 105–122.

Dong, G., Hutagalung, A.H., Fu, C., Novick, P., and Reinisch, K.M. (2005). The structures of exocyst subunit Exo70p and the Exo84p C-terminal domains reveal a common motif. Nat. Struct. Mol. Biol. **12:** 1094–1100.

EauClaire, S., and Guo, W. (2003). Conservation and specialization: The role of the exocyst in neuronal exocytosis. Neuron **3:** 369–370.

Elias, M., Drdova, E., Ziak, D., Bavlnka, B., Hala, M., Cvrckova, F., Soukupova, H., and Zarsky, V. (2003). The exocyst complex in plants. Cell Biol. Int. **27:** 199–201.

Eubel, H., Braun, H.P., and Millar, A.H. (2005). Blue-native PAGE in plants: A tool in analysis of protein-protein interactions. Plant Methods. **1:** 11.

Finger, F.P., and Novick, P. (1997). Sec3p is involved in secretion and morphogenesis in *Saccharomyces cerevisiae.* Mol. Biol. Cell **8:** 647–662.

Friedrich, G.A., Hildebrand, J.D., and Soriano, P. (1997). The secretory protein Sec8 is required for paraxial mesoderm formation in the mouse. Dev. Biol. **2:** 364–374.

Garrick, M.D., and Garrick, L.M. (2007). Loss of rapid transferrin receptor recycling due to a mutation in Sec15/1 in hbd mice. Biochim. Biophys. Acta **1773:** 105–108.

Guo, W., Grant, A., and Novick, P. (1999a). Exo84p is an exocyst protein essential for secretion. J. Biol. Chem. **33:** 23558–23564.

Guo, W., Roth, D., Walch-Solimena, C., and Novick, P. (1999b). The exocyst is an effector for Sec4p, targeting secretory vesicles to sites of exocytosis. EMBO J. **4:** 71–80.

Guo, W., Tamanoi, F., and Novick, P. (2001). Spatial regulation of the exocyst complex by Rho1 GTPase. Nat. Cell Biol. **3:** 353–360.

Hamburger, Z.A., Hamburger, A.E., West, A.P., and Weis, W.I. (2006). Crystal structure of the *S. cerevisiae* exocyst component Exo70p. J. Mol. Biol. **356:** 9–21.

Hazuka, C.D., Foletti, D.L., Hsu, S.C., Kee, Y., Hopf, F.W., and Scheller, R.H. (1999). The sec6/8 complex is located at neurite outgrowth and axonal synapse-assembly domains. J. Neurosci. **4:** 324–334.

Hsu, S.C., Hazuka, C.D., Foletti, D.L., Heuser, J., and Scheller, R.H. (1998). Subunit composition, protein interactions and structures of the mammalian brain sec6/8 complex and septin filaments. Neuron **20:** 1111–1122.

Hsu, S.C., TerBush, D., Abraham, M., and Guo, W. (2004). The exocyst complex in polarized exocytosis. Int. Rev. Cytol. **233:** 243–265.

Hsu, S.C., Ting, A.E., Hazuka, C.D., Davanger, S., Kenny, J.W., Kee, Y., and Scheller, R.H. (1996). The mammalian brain rsec6/8 complex. Neuron **6:** 209–219.

Jafar-Nejad, H., Andrews, H.K., Acar, M., Bayat, V., Wirtz-Peitz, F., Mehta, S.Q., Knoblich, J.A., and Bellen, H.J. (2005). Sec15, a component of the exocyst, promotes notch signaling during the asymmetric division of Drosophila sensory organ precursors. Dev. Cell **9:** 351–363.

Johnson-Brousseau, S., and McCormick, S. (2004). A compendium of methods useful for characterizing *Arabidopsis* pollen mutants and gametophytically expressed genes. Plant J. **39:** 761–775.

Jurgens, G., and Geldner, N. (2002). Protein secretion in plants: from the trans-Golgi network to the outer space. Traffic **3:** 605–613.

Kee, Y., Yoo, J.S., Hazuka, C.D., Peterson, K.E., Hsu, S.C., and Scheller, R.H. (1997). Subunit structure of the mammalian exocyst complex. Proc. Natl. Acad. Sci. USA **94:** 14438–14443.

Koumandou, V.L., Dacks, J.B., Coulson, R.M., and Field, M.C. (2007). Control systems for membrane fusion in the ancestral eukaryote: Evolution of tethering complexes and SM proteins. BMC Evol. Biol. **7:** 29.

Lavy, M., Bloch, D., Hazak, O., Gutman, I., Poraty, L., Sorek, N., Sternberg, H., and Yalovsky, S.A. (2007). Novel ROP/RAC effector links cell polarity, root-meristem maintenance, and vesicle trafficking. Curr. Biol. **17:** 947–952.

Li, C.R., Lee, R.T., Wang, Y.M., Zheng, X.D., and Wang, Y. (2007). *Candida albicans* hyphal morphogenesis occurs in Sec3p-independent and Sec3p-dependent phases separated by septin ring formation. J. Cell Sci. **120:** 1898–1907.

Lim, J.E., Jin, O., Bennett, C., Morgan, K., Wang, F., Trenor III, C.C., Fleming, M.D., and Andrews, N.C. (2005). A mutation in Sec15/1 causes anemia in hemoglobin deficit (hbd) mice. Nat. Genet. **37:** 1270–1273.

Matern, H.T., Yeaman, C., Nelson, W.J., and Scheller, R.H. (2001). The Sec6/8 complex in mammalian cells: characterization of mammalian Sec3, subunit interactions, and expression of subunits in polarized cells. Proc. Natl. Acad. Sci. USA **98:** 9648–9653.

Moore, B.A., Robinson, H.H., and Xu, Z. (2007). The crystal structure of mouse Exo70 reveals unique features of the mammalian exocyst. J. Mol. Biol. **371:** 410–421.

Moskalenko, S., Henry, D.O., Rosse, C., Mirey, G., Camonis, J.H., and White, M.A. (2002). The exocyst is a Ral effector complex. Nat. Cell Biol. **4:** 66–72.

Moskalenko, S., Tong, C., Rosse, C., Mirey, G., Formstecher, E., Daviet, L., Camonis, J., and White, M.A. (2003). Ral GTPases regulate exocyst assembly through dual subunit interactions. J. Biol. Chem. **278:** 51743–51748.

Munson, M., and Novick, P. (2006). The exocyst defrocked, a framework of rods revealed. Nat. Struct. Mol. Biol. **13:** 577–581.

Murthy, M., Garza, D., Scheller, R.H., and Schwarz, T.L. (2003). Mutations in the exocyst component Sec5 disrupt neuronal membrane traffic, but neurotransmitter release persists. Neuron **37:** 433–447.

Novick, P., Field, C., and Schekman, R. (1980). Identification of 23 complementation groups required for post-translational events in the yeast secretory pathway. Cell **21:** 205–215.

Otegui, M.S., and Staehelin, L.A. (2004). Electron tomographic analysis of post-meiotic cytokinesis during pollen development in *Arabidopsis thaliana.* Planta **218:** 501–515.

Perkins, D.N., Pappin, D.J., Creasy, D.M., and Cottrell, J.S. (1999). Probability-based protein identification by searching sequence databases using mass spectrometry data. Electrophoresis **20:** 3551–3567.

Pommereit, D., and Wouters, F.S. (2007). An NGF-induced Exo70-TC10 complex locally antagonises Cdc42-mediated activation of N-WASP to modulate neurite outgrowth. J. Cell Sci. **120:** 2694–2705.

Preuss, D., Rhee, S.Y., and Davis, R.W. (1994). Tetrad analysis possible in *Arabidopsis* with mutation of the QUARTET (QRT) genes. Science **264:** 1458–1460.

Prigent, M., Dubois, T., Raposo, G., Derrien, V., Tenza, D., Rossé, C., Camonis, J., and Chavrier, P. (2003). ARF6 controls post-endocytic recycling through its downstream exocyst complex effector. J. Cell Biol. **163:** 1111–1121.

Robinson, N.G., Guo, L., Imai, J., Toh-E, A., Matsui, Y., and Takanou, F. (1999). Rho3 of *Saccharomyces cerevisiae*, which regulates the actin cytoskeleton and exocytosis, is a GTPase which interacts with Myo2 and Exo70. Mol. Cell. Biol. **19:** 3580–3587.

Rosse, C., Hatzoglou, A., Parrini, M.C., White, M.A., Chavrier, P.,

and Camonis, J. (2006). RalB mobilizes the exocyst to drive cell migration. Mol. Cell. Biol. **26:** 727–734.

Rosso, M.G., Li, Y., Strizhov, N., Reiss, B., Dekker, K., and Weisshaar, B. (2003). An *Arabidopsis thaliana* T-DNA mutagenized population (GABI-Kat) for flanking sequence tag-based reverse genetics. Plant Mol. Biol. **53:** 247–259.

Roth, D., Guo, W., and Novick, P. (1998). Dominant-negative alleles of SEC10 reveal distinct domains involved in secretion and morphogenesis in yeast. Mol. Biol. Cell **7:** 725–739.

Schägger, H., and von Jagow, G. (1991). Blue native electrophoresis for isolation of membrane protein complexes in enzymatically active form. Anal. Biochem. **199:** 223–231.

Segui-Simarro, J.M., Austin II, J.R., White, E.A., and Staehelin, L.A. (2004). Electron tomographic analysis of somatic cell plate formation in meristematic cells of *Arabidopsis* preserved by high-pressure freezing. Plant Cell **16:** 836–856.

Sivaram, M.V., Furgason, M.L., Brewer, D.N., and Munson, M. (2006). The structure of the exocyst subunit Sec6p defines a conserved architecture with diverse roles. Nat. Struct. Mol. Biol. **13:** 555–556.

Sivaram, M.V., Saporita, J.A., Furgason, M.L., Boettcher, A.J., and Munson, M. (2005). Dimerization of the exocyst protein Sec6p and its interaction with the t-SNARE Sec9p. Biochemistry **44:** 6302–6311.

Synek, L., Schlager, N., Elias, M., Quentin, M., Hauser, M.T., and Zarsky, V. (2006). At EXO70A1, a member of a family of putative exocyst subunits specifically expanded in land plants, is important for polar growth and plant development. Plant J. **48:** 54–72.

Sztul, E., and Lupashin, V. (2006). Role of tethering factors in secretory membrane traffic. Am. J. Physiol. Cell Physiol. **290:** C11–C26.

Terbush, D.R., Guo, W., Dunkelbarger, S., and Novick, P. (2001). Purification and characterization of yeast exocyst complex. Methods Enzymol. **329:** 100–110.

TerBush, D.R., Maurice, T., Roth, D., and Novick, P. (1996). The exocyst is a multiprotein complex required for exocytosis in *Saccharomyces cerevisiae.* EMBO J. **15:** 6483–6494.

TerBush, D.R., and Novick, P. (1995). Sec6, Sec8, and Sec15 are components of a multisubunit complex which localizes to small bud tips in *Saccharomyces cerevisiae.* J. Cell Biol. **130:** 299–312.

Vega, I.E., and Hsu, S.C. (2001). The exocyst complex associates with microtubules to mediate vesicle targeting and neurite outgrowth. J. Neurosci. **21:** 3839–3848.

Wen, T.J., Hochholdinger, F., Sauer, M., Bruce, W., and Schnable, P.S. (2005). The roothairless1 gene of maize encodes a homolog of sec3, which is involved in polar exocytosis. Plant Physiol. **138:** 1637–1643.

Wen, T.J., and Schnable, P.S. (1994). Analyses of mutants of three genes that influence root hair development in *Zea mays* (Gramineae) suggest that root hairs are dispensable. Am. J. Bot. **81:** 833–842.

Werhahn, W., and Braun, H.P. (2002). Biochemical dissection of the mitochondrial proteome from *Arabidopsis thaliana* by three-dimensional gel electrophoresis. Electrophoresis **23:** 640–646.

Whyte, J.R., and Munro, S. (2001). The Sec34/35 Golgi transport complex is related to the exocyst, defining a family of complexes involved in multiple steps of membrane traffic. Dev. Cell **1:** 527–537.

Whyte, J.R., and Munro, S. (2002). Vesicle tethering complexes in membrane traffic. J. Cell Sci. **115:** 2627–2637.

Wu, S., Mehta, S.Q., Pichaud, F., Bellen, H.J., and Quiocho, F.A. (2005). Sec15 interacts with Rab11 via a novel domain and affects Rab11 localization in vivo. Nat. Struct. Mol. Biol. **12:** 879–885.

Yang, Z. (2002). Small GTPases: Versatile signaling switches in plants. Plant Cell **14:** S375–S388.

Yeaman, C. (2003). Ultracentrifugation-based approaches to study regulation of Sec6/8 (exocyst) complex function during development of epithelial cell polarity. Methods **30:** 198–206.

Yeaman, C., Grindstaff, K.K., and Nelson, W.J. (2004). Mechanism of recruiting Sec6/8 (exocyst) complex to the apical junctional complex during polarization of epithelial cells. J. Cell Sci. **117:** 559–570.

Zhang, X., Bi, E., Novick, P., Du, L., Kozminski, K.G., Lipschutz, J.H., and Guo, W. (2001). Cdc42 interacts with the exocyst and regulates polarized secretion. J. Biol. Chem. **276:** 46745–46750.

Zhang, X.M., Ellis, S., Sriratana, A., Mitchell, C.A., and Rowe, T. (2004). Sec15 is an effector for the Rab11 GTPase in mammalian cells. J. Biol. Chem. **279:** 43027–43034.

Zuo, X., Zhang, J., Zhang, Y., Hsu, S.C., Zhou, D., and Guo, W. (2006). Exo70 interacts with the Arp2/3 complex and regulates cell migration. Nat. Cell Biol. **8:** 1383–1388.